





Article

# Selenium(IV) Polybromide Complexes: Structural Diversity Driven by Halogen and Chalcogen Bonding

 Nikita A. Korobeynikov <sup>1</sup>, Andrey N. Usoltsev <sup>1</sup>, Alexander S. Novikov <sup>2,3</sup>, Pavel A. Abramov <sup>1</sup>, Maxim N. Sokolov <sup>1</sup> and Sergey A. Adonin <sup>1,\*</sup>
<sup>1</sup> Nikolaev Institute of Inorganic Chemistry SB RAS, 630090 Novosibirsk, Russia

<sup>2</sup> Institute of Chemistry, Saint Petersburg State University, 199034 Saint Petersburg, Russia

<sup>3</sup> Joint Research Institute of Chemistry, Faculty of Physics, Mathematics and Natural Sciences, People's Friendship University of Russia (RUDN University), 117198 Moscow, Russia

\* Correspondence: adonin@niic.nsc.ru

**Abstract:** Reactions between bromoselenate(IV)-containing solutions, dibromine and salts of pyridinium-family organic cations resulted in structurally diverse, bromine-rich polybromine-bromoselenates(IV): (4-MePyH)<sub>5</sub>[Se<sub>2</sub>Br<sub>9</sub>][SeBr<sub>6</sub>](Br<sub>3</sub>)<sub>2</sub> (**1**), (2-MePyH)<sub>2</sub>{[SeBr<sub>6</sub>](Br<sub>2</sub>)} (**2**), (PyH)<sub>2</sub>{[SeBr<sub>5</sub>]Br(Br<sub>2</sub>)<sub>2</sub>} (**3**), (1-MePy)<sub>2</sub>{[SeBr<sub>6</sub>](Br<sub>2</sub>)} (**4**). The compounds feature halogen and (in the case of **3**) chalcogen bonding in solid state, resulting in formation of supramolecular architectures of different dimensionality. DFT calculations allowed estimation of the energies of non-covalent interactions in **1–4**; additionally, characterization by Raman spectroscopy was performed.

**Keywords:** polyhalogens; halogen bonding; non-covalent interactions; selenium; chalcogen bonding



**Citation:** Korobeynikov, N.A.; Usoltsev, A.N.; Novikov, A.S.; Abramov, P.A.; Sokolov, M.N.; Adonin, S.A. Selenium(IV) Polybromide Complexes: Structural Diversity Driven by Halogen and Chalcogen Bonding. *Molecules* **2022**, *27*, 5355. <https://doi.org/10.3390/molecules27165355>

Academic Editor: Ting Wang

Received: 1 August 2022

Accepted: 17 August 2022

Published: 22 August 2022

**Publisher's Note:** MDPI stays neutral with regard to jurisdictional claims in published maps and institutional affiliations.



**Copyright:** © 2022 by the authors. Licensee MDPI, Basel, Switzerland. This article is an open access article distributed under the terms and conditions of the Creative Commons Attribution (CC BY) license (<https://creativecommons.org/licenses/by/4.0/>).

## 1. Introduction

Ability of homo- or heteroleptic halide complexes to form associates with di- or polyhalogens was discovered far before the formulation of the modern concepts of supramolecular chemistry (in particular, halogen bonding (XB), which stands beyond this phenomenon). Among the earliest examples, we can highlight the work by Petzold: [1] treating bromoantimonate(III) solutions by dibromine in presence of salts of different organic cations (mostly of pyridinium family), he isolated dark crystalline solids with unusually high bromine content (such as “SbBr<sub>9</sub>”) and confirmed the presence of polybromide species in these matters via redox titration. Later, the progress in XRD techniques allowed the group of researchers from the University of Iowa to re-discover these compounds: following from the structural data, bromoantimonate anions were accompanied by dibromine [2] or tribromide [3,4] units. The authors noticed unusually short Br···Br distances in these structures. At the same time, similar observations were made by von Schnering et al. [5] while working with tungsten bromide clusters. Since then, there appeared dozens of examples of crystal structures featuring halide ligand···polyhalogen interactions, but this information remained “unsorted” until 2018, when we presented a review on this topic [6]. The appearance of this summary followed the interest on polyhalogen-halometalates, which increased over the last decade. The works by the group of Feldmann [7–10] and Shevelkov [11–13], as well as our team [14–16], clearly revealed that ability to form supramolecular associates with di- or polyhalogens in solid state is rather common for halometalates of d- and, especially, p-block elements. Diversity of such compounds is especially rich in the case of iodine- and bromine-rich substances, but corresponding complexes can be obtained also with dichlorine (after the very first work by Weiss et al. [17], we recently provided additional examples of dichlorine-chlorometalates, as well as theoretical insights into the nature of Cl<sub>2</sub> bonding in these substances [18,19]).

Currently, polyhalogen-halometalates are known for many elements, including metalloids (Te). In the course of our work, we were curious whether this chemistry can

be expanded towards the elements of the periodic table with even less metallic properties. For selenium, there are two examples [20,21] of dibromine-bromoselenates(IV) (both based on  $[\text{Se}_2\text{Br}_{10}]^{2-}$ ) as well as one dichlorine-containing complex reported by us very recently [22]. We decided to check whether 1) new representatives of the family of dibromine-bromoselenates can be prepared via the methods we utilized for Te(IV) derivatives and 2) if this idea works, how structurally similar or different from those of Te(IV) such complexes will be.

Hereby, we present four dibromine-bromoselenates(IV): (4-MePyH) $_5$ [Se $_2$ Br $_9$ ][SeBr $_6$ ](Br $_3$ ) $_2$  (**1**), (2-MePyH) $_2$ {[SeBr $_6$ ](Br $_2$ )} (**2**), (PyH) $_2$ {[SeBr $_5$ ]Br(Br $_2$ ) $_2$ } (**3**), (1-MePy) $_2$ {[SeBr $_6$ ](Br $_2$ )} (**4**).

## 2. Materials and Methods

All reagents were obtained from commercial sources and used as purchased. Solvents were purified according to the standard procedures. 1-methylpyridinium iodide (1-MePyI) was prepared by reaction of pyridine and methyl iodide (1:1.05) with nearly quantitative yield. In all cases, concentrated aqueous HBr was used. Caution: the work with dibromine and its solutions, as well as with concentrated HBr, requires obligatory use of fume hood and adequate eye and skin protection (goggles and gloves). Selenium dioxide is toxic; compounds **1–4** must be treated as toxic as well.

### 2.1. Synthesis of **1**

In total, 111 mg (1 mmol) of SeO $_2$  and 195  $\mu$ L (2 mmol) of 4-MePy were dissolved in 6 mL of HBr at 70 °C (30 min). After that, 1.59 g of Br $_2$  (10 mmol, 0.5 mL, 10 $\times$  excess to Se) were added dropwise, and the mixture was slowly cooled to r.t. Within several hours, reddish-black crystals of **1** were formed; yield was 69%.

### 2.2. Synthesis of **2**

In total, 55 mg (0.5 mmol) of SeO $_2$  and 99  $\mu$ L (1 mmol) of 2-MePy were dissolved in 6 mL of HBr at 70 °C (30 min). After that, 0.79 g of Br $_2$  (5 mmol, 0.25 mL, 10 $\times$  excess to Se) were added dropwise, and the mixture was slowly cooled to r.t. Within several hours, there form reddish-black crystals of **2**, decomposing rapidly while kept outside the dibromine-containing mother liquor (see Discussion).

### 2.3. Synthesis of **3**

The procedure was the same as for **2**, using pyridine (81  $\mu$ L, 1 mmol) instead of 2-MePy. Reddish-black crystals of **3**, decomposing rapidly while kept outside the dibromine-containing mother liquor (see Discussion), form within several hours after cooling the reaction mixture to r.t.

### 2.4. Synthesis of **4**

In total, 111 mg (0.5 mmol) of 1-MePyI were dissolved in 4 mL of water. After addition of 97 mg (0.58 mmol) of AgNO $_3$ , the mixture was stirred for 15 min. AgI was filtered off; to mother liquor, 2 mL of HBr was added and AgBr was filtered off. Solution was evaporated to dryness, and residue was dissolved in 3 mL of HBr, followed by the addition of 28 mg (0.25 mmol) of SeO $_2$ . The mixture was heated to 70 °C; then, 0.39 g (2.5 mmol, 0.13 mL) of Br $_2$  was added dropwise and the mixture was slowly cooled to r.t., resulting in the formation of dark cherry-red crystals of **4** within several hours. Yield was 79%. For C $_{12}$ H $_{16}$ Br $_8$ N $_2$ Se calcd, %: C, 16.01; H, 1.79; N, 3.11, found, %: C, 16.14, H, 1.90; N, 3.21.

### 2.5. X-ray Diffractometry

Crystallographic data and refinement details for **1–4** are given in Table S1 (Supplementary Materials). The diffraction data were collected on a Bruker D8 Venture diffractometer with a CMOS PHOTON III detector and I $\mu$ S 3.0 source (Mo K $\alpha$  radiation,  $\lambda = 0.71073$  Å) at 150 K. The  $\varphi$ - and  $\omega$ -scan techniques were employed. Absorption correction was applied by SADABS (Bruker Apex3 software suite: Apex3, SADABS-2016/2

and SAINT, version 2018.7–2; Bruker AXS Inc.: Madison, WI, USA, 2017). Structures were solved by SHELXT [23] and refined by full-matrix least-squares treatment against  $|F|^2$  in anisotropic approximation with SHELX 2014/7 [24] in ShelXle program [25]. *H*-atoms were refined in the geometrically calculated positions. The crystallographic data have been deposited in the Cambridge Crystallographic Data Centre under the deposition codes CCDC 2174852–2174855. These data can be obtained free of charge via [https://www.ccdc.cam.ac.uk/data\\_request/cif](https://www.ccdc.cam.ac.uk/data_request/cif), or by emailing [data\\_request@ccdc.cam.ac.uk](mailto:data_request@ccdc.cam.ac.uk).

### 2.6. Raman Spectroscopy

Raman spectra were collected using a LabRAM HR Evolution (Horiba) spectrometer with the excitation by the 633 nm line of the He-Ne laser. The spectra at room temperatures were obtained in the backscattering geometry with a Raman microscope. The laser beam was focused to a diameter of 2  $\mu\text{m}$  using a LMPlan FL 50 $\times$ /0.50 Olympus objective. The spectral resolution was 0.7  $\text{cm}^{-1}$ . The laser power on the sample surface was about 0.03 mW.

### 2.7. Powder X-ray Diffractometry (PXRD)

XRD analysis of polycrystals was performed on Shimadzu XRD-7000 diffractometer (CuK-alpha radiation, Ni-filter, linear One Sight detector, 0.0143 $^\circ$  2 $\theta$  step, 2 s per step). Plotting of PXRD patterns and data treatment was performed using X'Pert Plus software (see Supplementary Materials).

### 2.8. Thermogravimetric Analysis (TGA) and Computational Details

Details are given in Supplementary Materials.

## 3. Results and Discussion

Despite the general scheme of the preparation of polyhalogen-halometalates being rather simple (source of metal + source of halide, commonly taken as halide salt of organic cation + dihalogen), there are variations based on the choice of solvent. In some cases [7], ionic liquids were successfully used (this is a common approach in the synthesis of non-conventional polyhalogens [26–30]) for this purpose; additionally, organic solvents can be utilized. However, since we earlier found that combination of aqueous hydrohalic acids and metal oxide gives good results for  $M = \text{Bi, Te, Sb, Sn, etc.}$  [14,19], we decided to follow the same scheme for Se ( $\text{SeO}_2$  + concentrated aqueous  $\text{HBr} + \text{Br}_2$  + bromide salt of organic cation, see Section 2 for details). For **1–4**, it yields the formation of single crystals suitable for X-ray diffractometry.

The structural data for **1–4** demonstrate that Se(IV) can form the complexes similar to those with Te(IV), but this occurs not in all cases—Se(IV) derivatives are prominently more diverse in terms of supramolecular chemistry. In the structure of **1**, there are two types of bromoselenate(IV) anions in the structure—mononuclear  $[\text{SeBr}_6]^{2-}$  (Se-Br = 2.569–2.580  $\text{\AA}$ ) and binuclear  $[\text{Se}_2\text{Br}_9]^-$ . The latter type (two octahedra joint via one shared face) is very common for halometalates of Sb and Bi [31–38] but rare for Se [39,40]. The Sb-Br<sub>term</sub> bonds are 2.374–2.406  $\text{\AA}$ , while the Sb- $\mu_2$ -Br distances are expectedly longer (2.824–2.913  $\text{\AA}$ ). The longest Se $\cdots$ Br interactions (2.913  $\text{\AA}$ ) can also be regarded as strong chalcogen bonding, as follows from DFT calculations (see below). The tribromide anion is asymmetric (Br-Br = 2.467 and 2.668  $\text{\AA}$ ). The system of Br $\cdots$ Br non-covalent interactions (assuming their presence for the distances lesser than the sum of Bondi's van der Waals radii [41,42] for two Br atoms) is non-trivial. Each tribromide unit forms contacts with one  $[\text{SeBr}_6]^{2-}$  (via terminal Br; Br $\cdots$ Br = 3.432  $\text{\AA}$ ) and two  $[\text{Se}_2\text{Br}_9]^-$  anions (via central and terminal Br; Br $\cdots$ Br = 3.473 and 3.156  $\text{\AA}$ , respectively). Each  $[\text{Se}_2\text{Br}_9]^-$  interacts therefore with four Br<sub>3</sub><sup>−</sup> (Figure 1). Interestingly, the same composition of the anionic part was found in the salt described by Boyle et al. nearly two decades ago [40], but the system of non-covalent interactions in that case is not similar to the one in **1**.

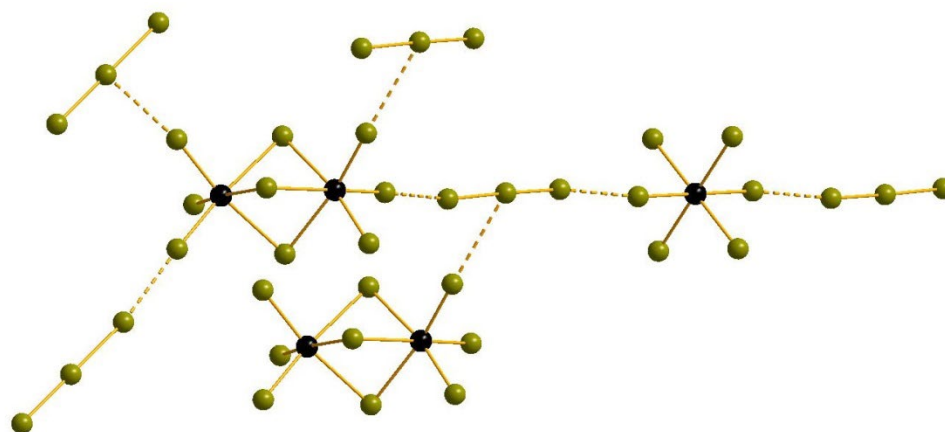


**Figure 1.** Br $\cdots$ Br non-covalent interactions in the structure of **1**. Here and below: Se, black; Br, olive-green; non-covalent contacts, dashed.

In  $[\text{SeBr}_6]^{2-}$  anions (Se-Br = 2.307–2.686 Å) in **2**, two bromide ligands are disordered over two positions each with 0.5 occupancy. The Br $_2$  units are disordered as well (0.5:0.5, Br-Br = 2.328–2.351 Å). The composition of **2** is very similar to most common for polybromo-bromotellurates(IV) [15] (one Br $_2$  per one octahedral  $[\text{MBr}_6]^{2-}$ ), but the system of Br $\cdots$ Br non-covalent interactions is more sophisticated. For one of Br $_2$  units, there is only one type of contacts which has the pattern identical to one found in polybromo-bromotellurates(IV)—it links bromoselenate(IV) anions and Br $_2$  (Br $\cdots$ Br = 3.110 Å) into 1D linear chains with Br $_{\text{term}}$ -Br $_{\text{Br}_2}$ -Br $_{\text{Br}_2}$  angle close to 180° (170.32°). For another Br $_2$  position, there are two types of interactions—one is the same as described above (Br $\cdots$ Br = 3.289 Å, Br-Br-Br = 174.52°), while another involves the bromide ligands of  $[\text{SeBr}_6]^{2-}$  of neighboring layer in packing (Br $\cdots$ Br = 3.359 Å) so that the Br-Br-Br angles are lower (111.74°) and a pseudo-3D structure is formed (Figure 2).

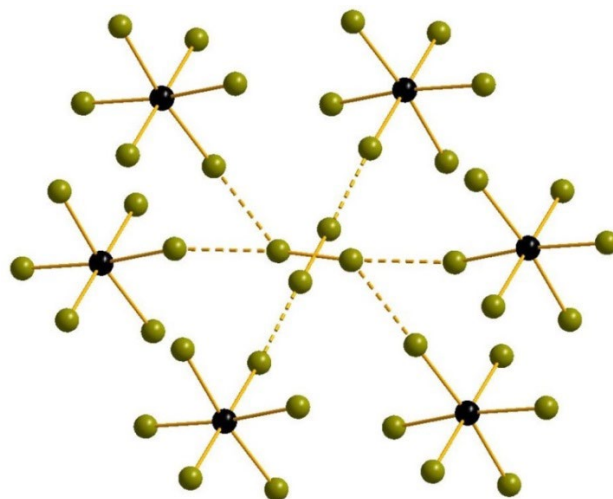


**Figure 2.** Br $\cdots$ Br interactions in the structure of **2**. Only one position of disordered bromide ligands is shown.

The structure of **3** (Figure 3) features the presence of pyramidal  $[\text{SeBr}_5]^-$  anions (Se-Br $_{\text{eq}}$  and Se-Br $_{\text{ax}}$  = 2.559 and 2.360 Å, respectively). Additionally, there are bromide anions which make coordination environment of Se pseudo-octahedral, but the Se $\cdots$ Br distances are too long for conventional covalent bonds (3.049 Å). Each of these Br $^-$  interacts with four Br $_2$  (Br-Br = 2.359 Å) units (Br $\cdots$ Br = 3.131 Å) and, additionally, with an axial bromide ligand of neighboring  $[\text{SeBr}_5]^-$  (Br $\cdots$ Br = 3.238 Å). An interesting feature of this structure is that the Br $\cdots$ Br distances between the equatorial Br ligands of  $[\text{SeBr}_5]^-$  anions are also shorter

than the sum of van der Waals radii (3.225 Å). Very similar effect was previously described for bromoantimonates(V) [16], where the system of such hypothetical interactions can be 1D, 2D, or even 3D. It is assumed that those can be responsible for enhanced photophysical behavior of some Cat[SbBr<sub>6</sub>] salts, which were utilized as light absorbers in model solar cells [43].

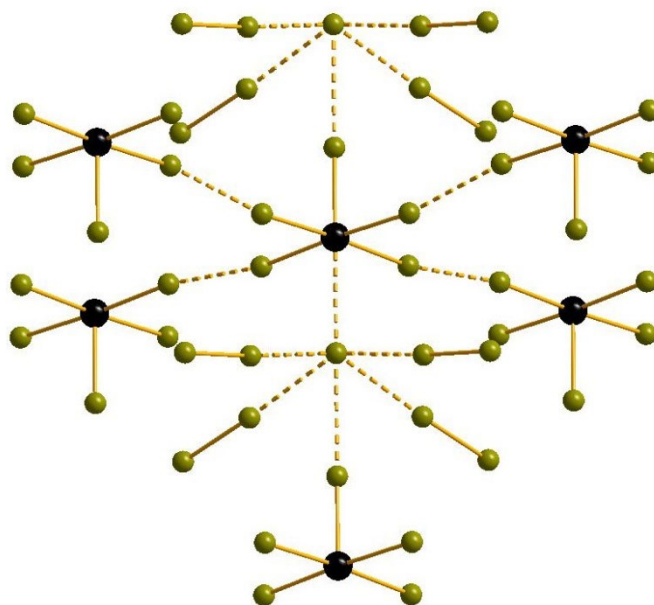


**Figure 3.** The system of non-covalent interactions in the structure of **3**.

Finally, complex **4** is isostructural to the tellurium-containing one-(1-MePy)<sub>2</sub>{[TeBr<sub>6</sub>](Br<sub>2</sub>)} [15]. The [SeBr<sub>6</sub>]<sup>2-</sup> (Se-Br = 2.513–2.610 Å) and Br<sub>2</sub> (Br-Br = 2.335 Å) units are linked (Br⋯Br = 3.143 Å, Br-Br-Br = 175.55°) into 1D linear chains (Figure 4).

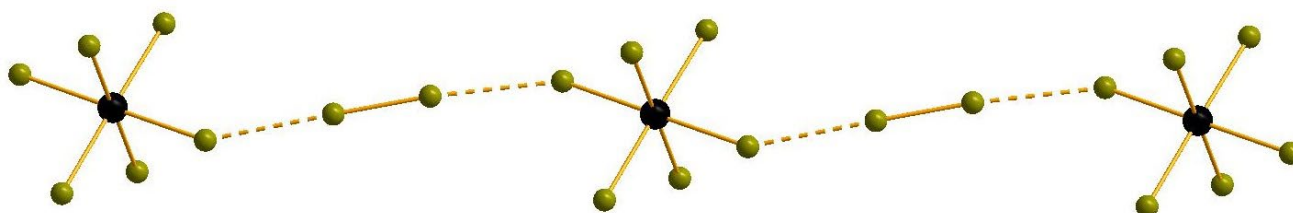


**Figure 4.** The system of non-covalent interactions in the structure of **4**.

Here, **1–4** demonstrate different stability while being kept outside the dibromine-containing mother liquor. Only **1** and **4** are stable enough for PXRD experiment (Figures S1 and S2); **1** is slightly contaminated by an unidentified minor byproduct, while **4** precipitates as a single phase. Moreover, **2** and **3** undergo decomposition with loss of Br<sub>2</sub> (detectable visually). However, we applied Raman spectroscopy for freshly isolated solids. In the case of **1** (Figure 5), the bands corresponding to asymmetric tribromide anion must appear in the 150–160 and 180–190 ranges [44,45], so those are likely overlapped by bromoselenate (150–180 cm<sup>-1</sup>) [46–48]. The bands of latter appear in spectrum of **2** at 150 and 161 cm<sup>-1</sup> (Figure 6), while Br<sub>2</sub> has highly characteristic mode at 250 cm<sup>-1</sup> (for Te(IV) derivatives [49], this band is at 265–271 cm<sup>-1</sup>). For **4**, the spectrum is very similar (Figure 7), but the Br<sub>2</sub> band appears at higher wavelength (268 cm<sup>-1</sup>). Finally, **3** has the least trivial spectrum (Figure 8). We assume that the band at 110 cm<sup>-1</sup> corresponds to [SeBr<sub>5</sub>]<sup>-</sup> anion, while strong bands at 244 and 268 cm<sup>-1</sup> are related to different Br<sub>2</sub> units in the structure.

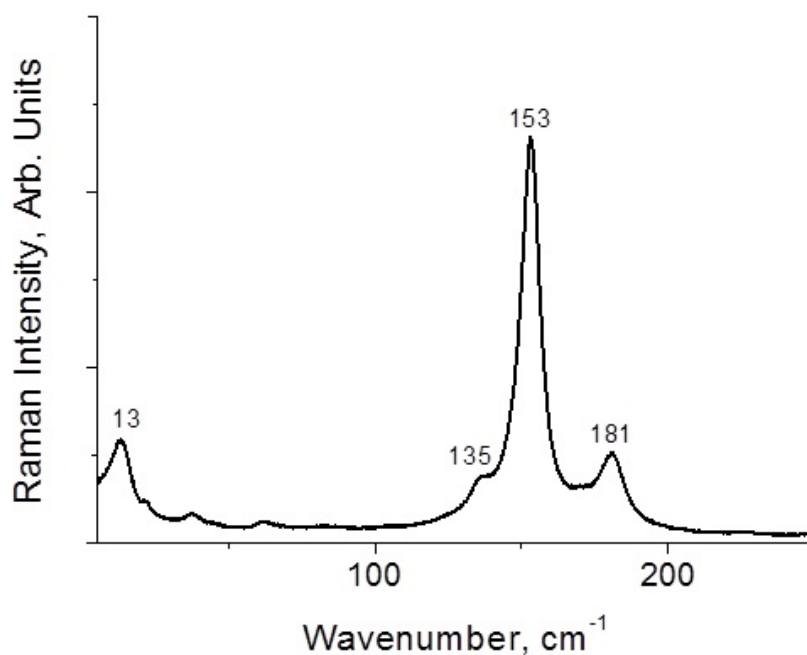


Figure 5. Raman spectrum of 1.

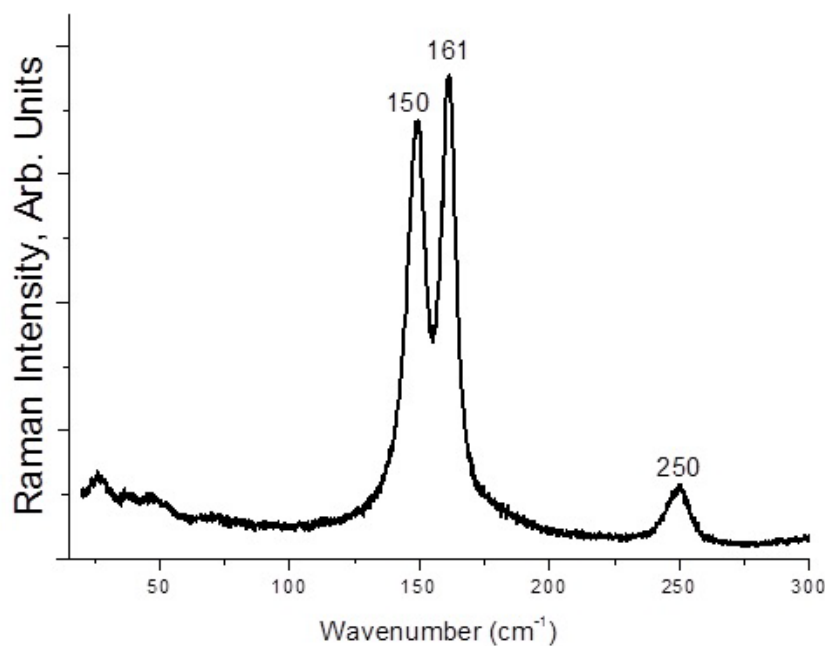


Figure 6. Raman spectrum of 2.

For theoretical investigation of the nature of non-covalent interactions in the above-mentioned complexes, we followed the approach which was extensively used by us for the examination of other relevant supramolecular systems: DFT calculations for non-optimized structures [50–54] (atomic coordinates extracted from XRD data) and QTAIM analysis [55] of electron density distribution. Unfortunately, disordering in the structure of **2** did not allow to perform analysis for this compound. For **1**, **3**, and **4**, results are summarized in Table 1 (see Supplementary Materials for graphical representation). Several interesting observations can be made. First, the energies of Br⋯Br interactions between the [SbBr<sub>5</sub>]<sup>−</sup> units in **3** are comparable with those of contacts with polyhalogen units, and this is very similar to the situation in polybromo-bromoantimonates(V) [16]. Most likely, this feature is general for halometalates with a high charge of the central atom. Second, the Se⋯Br interaction in **3**

is truly non-covalent ( $-G(r)/V(r) \geq 1$ ) [56], so it must be considered as chalcogen bonding. Third, all interactions in abovementioned structures are attractive [57,58]. The energies (up to 3.6 kcal/mol for Br $\cdots$ Br) are within the ranges typical for the compounds of this family.

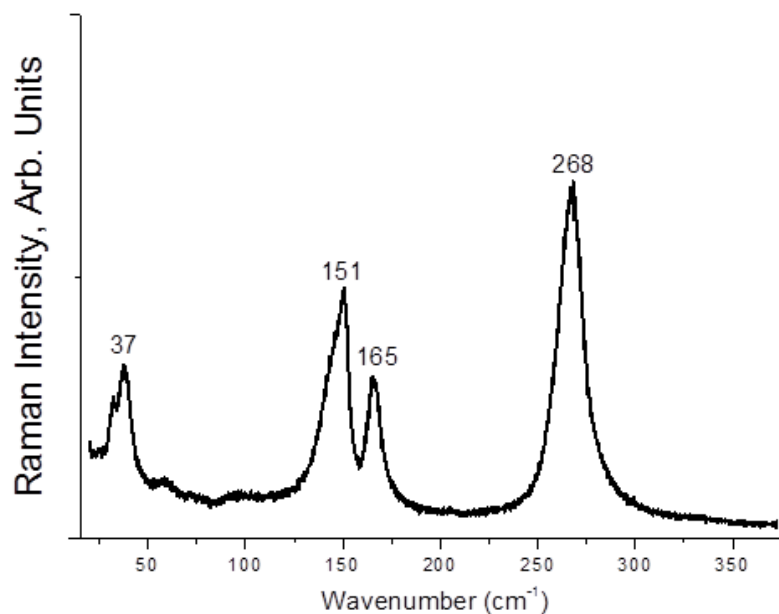


Figure 7. Raman spectrum of 4.

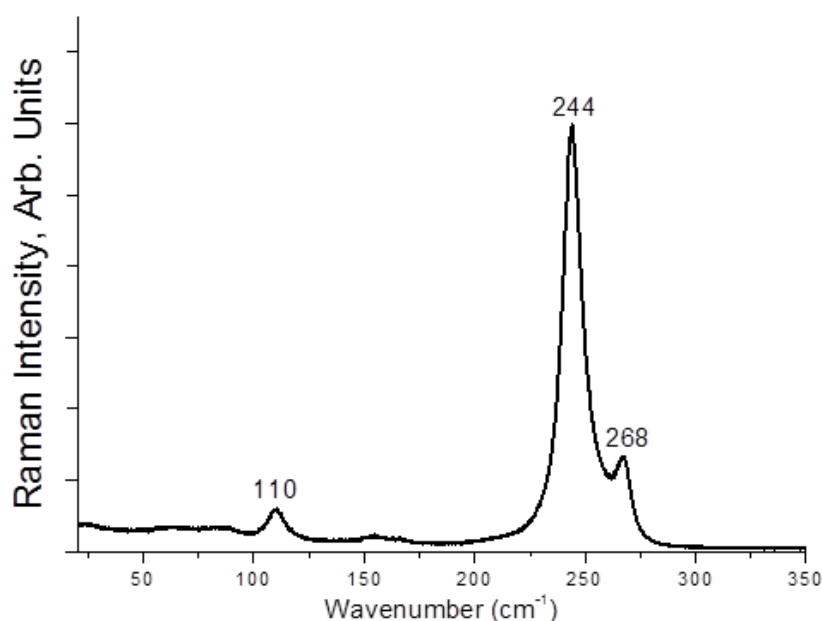


Figure 8. Raman spectrum of 3.

Since PXRD (see Supplementary Materials) indicates the permanent presence of minor impurities in 1 and since 2 and 3 are, as mentioned above, unstable, we performed TGA only for the last complex. Results are summarized in Supplementary Materials (Figure S3); thermal decomposition corresponding to the loss of dibromine unit (this pathway is common for the complexes of this sort) occurs at >100 °C, followed by complete destruction with total mass loss at >250 °C.

**Table 1.** Values of the density of all electrons  $\rho(\mathbf{r})$ , Laplacian of electron density  $\nabla^2\rho(\mathbf{r})$  and appropriate  $\lambda_2$  eigenvalues, energy density  $H_b$ , potential energy density  $V(\mathbf{r})$ , and Lagrangian kinetic energy  $G(\mathbf{r})$ , electron localization function ELF (a.u.) at the bond critical points (3, -1) for intermolecular interactions in **1**, **3**, **4**, and their estimated strength  $E_{\text{int}}$  (kcal/mol).

Contact	% of $\Sigma$ (vdW radii)	$\rho(\mathbf{r})$	$\nabla^2\rho(\mathbf{r})$	$-\lambda_2$	$H_b$	$-V(\mathbf{r})$	$G(\mathbf{r})$	ELF	$E_{\text{int}}^a$
<b>1</b>									
Br...Br 3.432 Å	94	0.011	0.027	0.011	0.000	0.006	0.006	0.053	2.2
Br...Br 3.156 Å	86	0.017	0.044	0.017	0.001	0.009	0.010	0.094	3.3
Br...Br 3.473 Å	95	0.011	0.028	0.011	0.001	0.006	0.007	0.047	2.2
Se...Br 2.913 Å	78	0.031	0.080	0.031	0.001	0.021	0.020	0.157	7.6
<b>3</b>									
Se...Br 3.049 Å	82	0.024	0.052	0.024	0.001	0.012	0.013	0.175	4.4
Br...Br 3.225 Å	88	0.015	0.041	0.015	0.001	0.009	0.010	0.074	3.3
Br...Br 3.238 Å	88	0.016	0.036	0.016	0.000	0.008	0.008	0.111	2.9
Br...Br 3.131 Å	86	0.020	0.046	0.020	0.001	0.010	0.011	0.131	3.6
<b>4</b>									
Br...Br 3.143 Å	86	0.019	0.042	0.019	0.001	0.009	0.010	0.133	3.3

<sup>a</sup>  $E_{\text{int}} = 0.58(-V(\mathbf{r}))$  (this empirical correlation between the interaction energy and the potential energy density of electrons at the bond critical points (3, -1) was specifically developed for non-covalent interactions involving bromine atoms) [59].

#### 4. Conclusions

We demonstrated that selenium can form extensive family of polybromo-bromoselenates (IV), which can be structurally different from corresponding Te (IV) derivatives. The nature of this element enables formation of non-covalent interactions between the bromide ligands of neighboring  $[\text{SeBr}_5]^-$  units, similar to how it occurs in Sb (V) complexes. Besides, unlike Te (IV), selenium can participate in formation of chalcogen bonding in these compounds.

**Supplementary Materials:** The following supporting information can be downloaded at: <https://www.mdpi.com/article/10.3390/molecules27165355/s1>, XRD, PXRD, and TGA data, as well as computational details.

**Author Contributions:** Conceptualization, S.A.A. and M.N.S.; methodology, S.A.A.; validation, P.A.A. and A.N.U.; formal analysis, S.A.A., A.S.N. and P.A.A.; investigation, N.A.K., A.S.N. and P.A.A.; resources, S.A.A.; data curation, A.N.U. and A.S.N.; writing—original draft preparation, S.A.A., A.N.U., P.A.A. and A.S.N.; writing—review and editing, M.N.S.; visualization, N.A.K. and S.A.A.; supervision, M.N.S. and S.A.A.; project administration, S.A.A.; funding acquisition, S.A.A. All authors have read and agreed to the published version of the manuscript.

**Funding:** This research was funded by the Russian Science Foundation, Grant No. 18-73-10040, and partially supported by the Ministry of Science and Higher Education of the Russian Federation (spectral characterization of the samples, 121031700313-8). A.S.N. is grateful to the RUDN University Strategic Academic Leadership Program.

**Institutional Review Board Statement:** Not applicable.

**Informed Consent Statement:** Not applicable.

**Data Availability Statement:** Not applicable.

**Conflicts of Interest:** The authors declare no conflict of interest.

**Sample Availability:** Samples of the compounds are not available from the authors.



## References

1. Petzold, W. Komplexe Bromverbindungen des Antimons. *Z. Anorg. Allg. Chem.* **1933**, *215*, 92–102. [[CrossRef](#)]
2. Hubbard, C.R.; Jacobson, R.A. Molecular bromine bridging of SbIII2Br9<sup>3-</sup> anions and the crystal structure of tetraethylammonium nonabromodiantimonate(III)-dibromine. *Inorg. Chem.* **1972**, *11*, 2247–2250. [[CrossRef](#)]
3. Lawton, S.L.; McAfee, E.R.; Benson, J.E.; Jacobson, R.A. Crystal structure of quinolinium hexabromoantimonate(V) tribromide, (C<sub>9</sub>H<sub>7</sub>NH)<sub>2</sub>SbVBr<sub>9</sub>. *Inorg. Chem.* **1973**, *12*, 2939–2944. [[CrossRef](#)]
4. Lawton, S.L.; Jacobson, R.A. Crystal structure of di- $\alpha$ -picolinium nonabromoantimonate(V). *Inorg. Chem.* **1968**, *7*, 2124–2134. [[CrossRef](#)]
5. Siepmann, R.; von Schnering, H.G. Die Kristallstruktur von W<sub>6</sub>Br<sub>16</sub>. Eine Verbindung mit Polykationen [W<sub>6</sub>Br<sub>8</sub>]<sup>6+</sup> und Polyanionen [Br<sub>4</sub>]<sup>2-</sup>. *ZAAC-J. Inorg. Gen. Chem.* **1968**, *357*, 289–298. [[CrossRef](#)]
6. Adonin, S.A.; Sokolov, M.N.; Fedin, V.P. Polyhalide-bonded metal complexes: Structural diversity in an eclectic class of compounds. *Coord. Chem. Rev.* **2018**, *367*, 1–17. [[CrossRef](#)]
7. Hausmann, D.; Feldmann, C. Bromine-rich Zinc Bromides: Zn<sub>6</sub>Br<sub>12</sub> (18-crown-6)<sub>2</sub> × (Br<sub>2</sub>)<sub>5</sub>, Zn<sub>4</sub>Br<sub>8</sub> (18-crown-6)<sub>2</sub> × (Br<sub>2</sub>)<sub>3</sub>, and Zn<sub>6</sub>Br<sub>12</sub> (18-crown-6)<sub>2</sub> × (Br<sub>2</sub>)<sub>2</sub>. *Inorg. Chem.* **2016**, *55*, 6141–6147. [[CrossRef](#)]
8. Eich, A.; Köppe, R.; Roesky, P.W.; Feldmann, C. Ionic-Liquid-Based Synthesis of the Bromine-Rich Bromidoplatinates [NBu<sub>3</sub>Me]<sub>2</sub>[Pt<sub>2</sub>Br<sub>10</sub>](Br<sub>2</sub>)<sub>2</sub> and [NBu<sub>3</sub>Me]<sub>2</sub>[Pt<sub>2</sub>Br<sub>10</sub>](Br<sub>2</sub>)<sub>3</sub>. *Z. Anorg. Allg. Chem.* **2018**, *644*, 275–279. [[CrossRef](#)]
9. Okrut, A.; Feldmann, C. {[P(o-tolyl)<sub>3</sub>]Br}<sub>2</sub>[Cu<sub>2</sub>Br<sub>6</sub>](Br<sub>2</sub>)<sub>n</sub> An Ionic Compound Containing Molecular Bromine. *Inorg. Chem.* **2008**, *47*, 3084–3087. [[CrossRef](#)]
10. Eich, A.; Köppe, R.; Roesky, P.W.; Feldmann, C. The Bromine-Rich Bromido Metallates [BMIm]<sub>2</sub>[SnBr<sub>6</sub>](Br<sub>2</sub>) and [MnBr(18-crown-6)]<sub>4</sub>[SnBr<sub>6</sub>]<sub>2</sub>(Br<sub>2</sub>)<sub>4.5</sub>. *Eur. J. Inorg. Chem.* **2019**, *2019*, 1292–1298. [[CrossRef](#)]
11. Shestimerova, T.A.; Golubev, N.A.; Yelavik, N.A.; Bykov, M.A.; Grigorieva, A.V.; Wei, Z.; Dikarev, E.V.; Shevelkov, A.V. Role of I<sub>2</sub> Molecules and Weak Interactions in Supramolecular Assembling of Pseudo-Three-Dimensional Hybrid Bismuth Polyiodides: Synthesis, Structure, and Optical Properties of Phenylenediammonium Polyiodobismuthate(III). *Cryst. Growth Des.* **2018**, *18*, 2572–2578. [[CrossRef](#)]
12. Mezentsev-Cherkes, I.A.; Shestimerova, T.A.; Medved'ko, A.V.; Kalinin, M.A.; Kuznetsov, A.N.; Wei, Z.; Dikarev, E.V.; Vatsadze, S.Z.; Shevelkov, A.V. Synthesis and supramolecular organization of the iodide and triiodides of a polycyclic adamantane-based diammonium cation: The effects of hydrogen bonds and weak I ··· I interactions. *CrystEngComm* **2021**, *23*, 2384–2395. [[CrossRef](#)]
13. Shestimerova, T.A.; Yelavik, N.A.; Mironov, A.V.; Kuznetsov, A.N.; Bykov, M.A.; Grigorieva, A.V.; Utochnikova, V.V.; Lepnev, L.S.; Shevelkov, A.V. From isolated anions to polymer structures through linking with i<sub>2</sub>: Synthesis, structure, and properties of two complex bismuth(III) iodine iodides. *Inorg. Chem.* **2018**, *57*, 4077–4087. [[CrossRef](#)] [[PubMed](#)]
14. Adonin, S.A.; Gorokh, I.D.; Novikov, A.S.; Samsonenko, D.G.; Plyusnin, P.E.; Sokolov, M.N.; Fedin, V.P. Bromine-rich complexes of bismuth: Experimental and theoretical studies. *Dalt. Trans.* **2018**, *47*, 2683–2689. [[CrossRef](#)]
15. Usoltsev, A.N.; Adonin, S.A.; Novikov, A.S.; Samsonenko, D.G.; Sokolov, M.N.; Fedin, V.P. One-dimensional polymeric polybromotellurates(IV): Structural and theoretical insights into halogen ··· halogen contacts. *CrystEngComm* **2017**, *19*, 5934–5939. [[CrossRef](#)]
16. Adonin, S.A.; Bondarenko, M.A.; Abramov, P.A.; Novikov, A.S.; Plyusnin, P.E.; Sokolov, M.N.; Fedin, V.P. Bromo- and Polybromoantimonates(V): Structural and Theoretical Studies of Hybrid Halogen-Rich Halometalate Frameworks. *Chem. A Eur. J.* **2018**, *24*, 10165–10170. [[CrossRef](#)]
17. Storck, P.; Weiss, A. <sup>35</sup>Cl NQR and X-Ray Studies of Hexachloropalladates A<sub>2</sub>PdCl<sub>6</sub> (A = Rb, Cs, NH<sub>4</sub>) and the Cl<sub>2</sub>-Clathrates Bis (tetramethylammonium) hexachloropalladate (Me<sub>4</sub>N)<sub>2</sub>PdCl<sub>6</sub> · Cl<sub>2</sub> and Bis (tetramethylammonium) hexachlorostannate (Me<sub>4</sub>N)<sub>2</sub>SnCl<sub>6</sub> · Cl<sub>2</sub>. *Z. Naturforsch. Sect. B J. Chem. Sci.* **1991**, *46*, 1214–1218. [[CrossRef](#)]
18. Usoltsev, A.N.; Adonin, S.A.; Kolesov, B.A.; Novikov, A.S.; Fedin, V.P.; Sokolov, M.N. Opening the third century of polyhalide chemistry: Thermally stable complex with “trapped” dichlorine. *Chem. A Eur. J.* **2020**, *26*, 13776–13778. [[CrossRef](#)]
19. Usoltsev, A.N.; Korobeynikov, N.A.; Kolesov, B.A.; Novikov, A.S.; Samsonenko, D.G.; Fedin, V.P.; Sokolov, M.N.; Adonin, S.A. Rule, Not Exclusion: Formation of Dichlorine-Containing Supramolecular Complexes with Chlorometalates(IV). *Inorg. Chem.* **2021**, *60*, 4171–4177. [[CrossRef](#)]
20. Janickis, V. Syntheses and Crystal Structures of Phenyltrimethylammonium salts of a mixed Hexabromoselenate/tellurate(IV), [C<sub>6</sub>H<sub>5</sub>(CH<sub>3</sub>)<sub>3</sub>N]<sub>2</sub>[Se 0.75Te0.25Br<sub>6</sub>], and a mixed catena-poly. *Acta Chem. Scand.* **1999**, *53*, 188–193. [[CrossRef](#)]
21. Hauge, S.; Marøy, K. Syntheses and crystal structures of phenyltrimethylammonium salts of hexabromoselenate(IV), [C<sub>6</sub>H<sub>5</sub>(CH<sub>3</sub>)<sub>3</sub>N]<sub>2</sub>[SeBr<sub>6</sub>], and catena-poly[(Di- $\mu$ -bromobis{tetrabromotellurate(IV)})- $\mu$ -bromine], [C<sub>6</sub>H<sub>5</sub>(CH<sub>3</sub>)<sub>3</sub>N]<sub>2n</sub>[Se<sub>2</sub>Br<sub>10</sub> · Br<sub>2</sub>]<sub>n</sub>. *Acta Chem. Scand.* **1996**, *50*, 399–404. [[CrossRef](#)]
22. Usoltsev, A.N.; Korobeynikov, N.A.; Kolesov, B.A.; Novikov, A.S.; Abramov, P.A.; Sokolov, M.N.; Adonin, S.A. Oxochloroselenate(IV) with Incorporated [Cl<sub>2</sub>]: The Case of Strong Cl ··· Cl Halogen Bonding. *Chem. A Eur. J.* **2021**, *27*, 9292–9294. [[CrossRef](#)]
23. Sheldrick, G.M. SHELXT—Integrated space-group and crystal-structure determination. *Acta Crystallogr. Sect. A Found. Adv.* **2015**, *71*, 3–8. [[CrossRef](#)]
24. Sheldrick, G.M. Crystal structure refinement with SHELXL. *Acta Crystallogr. Sect. C Struct. Chem.* **2015**, *71*, 3–8. [[CrossRef](#)] [[PubMed](#)]

25. Hübschle, C.B.; Sheldrick, G.M.; Dittrich, B. ShelXle: A Qt graphical user interface for SHELXL. *J. Appl. Crystallogr.* **2011**, *44*, 1281–1284. [[CrossRef](#)] [[PubMed](#)]
26. Wolff, M.; Okrut, A.; Feldmann, C. [(Ph)<sub>3</sub>PBr][Br<sub>7</sub>], [(Bz)(Ph)<sub>3</sub>P]<sub>2</sub>[Br<sub>8</sub>], [(n-Bu)<sub>3</sub>MeN]<sub>2</sub>[Br<sub>20</sub>], [C<sub>4</sub>MPyr]<sub>2</sub>[Br<sub>20</sub>], and [(Ph)<sub>3</sub>PCl]<sub>2</sub>[Cl<sub>2</sub>I<sub>4</sub>]: Extending the Horizon of Polyhalides via Synthesis in Ionic Liquids. *Inorg. Chem.* **2011**, *50*, 11683–11694. [[CrossRef](#)] [[PubMed](#)]
27. Wolff, M.; Meyer, J.; Feldmann, C. [C<sub>4</sub>MPyr]<sub>2</sub>[Br<sub>20</sub>]: Ionic-Liquid-Based Synthesis of a Three-Dimensional Polybromide Network. *Angew. Chem. Int. Ed.* **2011**, *50*, 4970–4973. [[CrossRef](#)]
28. Sonnenberg, K.; Pröhm, P.; Steinhauer, S.; Wiesner, A.; Müller, C.; Riedel, S. Formation and Characterization of [BrC(NMe<sub>2</sub>)<sub>2</sub>][Br<sub>3</sub>] and [BrC(NMe<sub>2</sub>)<sub>2</sub>]<sub>2</sub>[Br<sub>8</sub>] in Ionic Liquids. *Z. Anorg. Allg. Chem.* **2017**, *643*, 101–105. [[CrossRef](#)]
29. Haller, H.; Hog, M.; Scholz, F.; Scherer, H.; Krossing, I.; Riedel, S. [HMIM][Br<sub>9</sub>]: A Room-temperature Ionic Liquid Based on a Polybromide Anion. *Z. Naturforsch. B* **2013**, *68*, 1103–1107. [[CrossRef](#)]
30. Brückner, R.; Haller, H.; Steinhauer, S.; Müller, C.; Riedel, S. A 2D Polychloride Network Held Together by Halogen-Halogen Interactions. *Angew. Chem. Int. Ed.* **2015**, *54*, 15579–15583. [[CrossRef](#)]
31. Ahmed, I.A.; Blachnik, R.; Reuter, H. Synthesis and Thermal Behaviour of Compounds in the System [Ph<sub>4</sub>P]Cl/BiCl<sub>3</sub> and the Crystal Structures of [Ph<sub>4</sub>P]<sub>3</sub>[Bi<sub>2</sub>Cl<sub>9</sub>] · 2 CH<sub>2</sub>Cl<sub>2</sub> and [Ph<sub>4</sub>P]<sub>2</sub>[Bi<sub>2</sub>Cl<sub>8</sub>] · 2CH<sub>3</sub>COCH<sub>3</sub>. *Z. Anorg. Allg. Chem.* **2001**, *627*, 2057. [[CrossRef](#)]
32. Kulicka, B.; Lis, T.; Kinzhybalov, V.; Jakubas, R.; Piecha, A. Novel anionic water-containing inorganic fragment in [4-NH<sub>2</sub>PyH]<sub>8</sub>[Bi<sub>2</sub>Cl<sub>11</sub>] [Bi<sub>2</sub>Cl<sub>9</sub>(H<sub>2</sub>O)<sub>2</sub>]: Structural characterization, thermal, dielectric and vibrational properties. *Polyhedron* **2010**, *29*, 2014–2022. [[CrossRef](#)]
33. Szklarz, P.; Jakubas, R.; Piecha-Bisiorek, A.; Bator, G.; Chański, M.; Medycki, W.; Wuttke, J. Organic-inorganic hybrid crystals, (2,4,6-CH<sub>3</sub>PyH)<sub>3</sub>Sb<sub>2</sub>Cl<sub>9</sub> and (2,4,6-CH<sub>3</sub>PyH)<sub>3</sub>Bi<sub>2</sub>Cl<sub>9</sub>. Crystal structure characterization and tunneling of CH<sub>3</sub> groups studied by <sup>1</sup>H NMR and neutron spectroscopy. *Polyhedron* **2018**, *139*, 249–256. [[CrossRef](#)]
34. Wojtaś, M.; Jakubas, R.; Ciunik, Z.; Medycki, W. Structure and phase transitions in [(CH<sub>3</sub>)<sub>4</sub>P]<sub>3</sub>[Sb<sub>2</sub>Br<sub>9</sub>] and [(CH<sub>3</sub>)<sub>4</sub>P]<sub>3</sub>[Bi<sub>2</sub>Br<sub>9</sub>]. *J. Solid State Chem.* **2004**, *177*, 1575–1584. [[CrossRef](#)]
35. Wang, Y.-Y.; Song, L.; Dai, Z.-Q.; Xu, J.-C.; He, J.; Liu, W.; Shen, H.-Y.; Chai, W.-X. Synthesis, crystal structure, optoelectric properties and theoretical study of three perovskite-like iodobismuthate charge-transfer salts based on butylpyridinium. *J. Solid State Chem.* **2021**, *304*. [[CrossRef](#)]
36. Wojtaś, M.; Jakubas, R.; Baran, J. Vibrational study of the ferroelastic phase transition in [(CH<sub>3</sub>)<sub>4</sub>P]<sub>3</sub>[Bi<sub>2</sub>Cl<sub>9</sub>] and [(CH<sub>3</sub>)<sub>4</sub>P]<sub>3</sub>[Bi<sub>2</sub>Br<sub>9</sub>]. *Vib. Spectrosc.* **2005**, *39*, 23–30. [[CrossRef](#)]
37. Wang, Q.; Zhang, W.-Y.; Shi, P.-P.; Ye, Q.; Fu, D.-W. Switchable Dielectric Phase Transition Triggered by Pendulum-Like Motion in an Ionic Co-crystal. *Chem. Asian J.* **2018**, *13*, 2916–2922. [[CrossRef](#)]
38. Wang, P.; Chen, Z.R.; Li, H.H. Novel Viologen/Iodobismuthate Hybrids: Structures, Thermochromisms and Theoretical Calculations. *J. Clust. Sci.* **2020**, *31*, 943–950. [[CrossRef](#)]
39. Hammerschmidt, A.; Beckmann, I.; Läge, M.; Krebs, B. A Novel Crown-Ether Stabilized Oxonium Halogenochalcogenate(IV): [H<sub>7</sub>O<sub>3</sub> (Bis-dibromo-dibenzo-30-crown-10)][Se<sub>2</sub>Br<sub>9</sub>]<sub>1.5</sub>CH<sub>2</sub>Cl<sub>2</sub>. *Z. Naturforsch. Sect. B J. Chem. Sci.* **2004**, *59*, 1438–1443. [[CrossRef](#)]
40. Boyle, P.D.; Cross, W.I.; Godfrey, S.M.; McAuliffe, C.A.; Pritchard, R.G.; Teat, S.J. Reaction of dimethylselenourea and selenourea with dibromine to produce selenourea-dibromine, the 'T'-shaped 1:1 molecular adduct N,N-dimethyl-2-selenourea-dibromine, its solvent of crystallisation-containing analogue and the unusual ionic compound. *J. Chem. Soc. Dalton Trans.* **1999**, 2845–2852. [[CrossRef](#)]
41. Bondi, A. van der Waals Volumes and Radii of Metals in Covalent Compounds. *J. Phys. Chem.* **1966**, *70*, 3006–3007. [[CrossRef](#)]
42. Mantina, M.; Chamberlin, A.C.; Valero, R.; Cramer, C.J.; Truhlar, D.G. Consistent van der Waals Radii for the Whole Main Group. *J. Phys. Chem. A* **2009**, *113*, 5806–5812. [[CrossRef](#)] [[PubMed](#)]
43. Adonin, S.A.; Frolova, L.A.; Sokolov, M.N.; Shilov, G.V.; Korchagin, D.V.; Fedin, V.P.; Aldoshin, S.M.; Stevenson, K.J.; Troshin, P.A. Antimony (V) Complex Halides: Lead-Free Perovskite-Like Materials for Hybrid Solar Cells. *Adv. Energy Mater.* **2018**, *8*, 1701140. [[CrossRef](#)]
44. Haller, H.; Riedel, S. Recent Discoveries of Polyhalogen Anions—from Bromine to Fluorine. *Z. Anorg. Allg. Chem.* **2014**, *640*, 1281–1291. [[CrossRef](#)]
45. Evans, J.C.; Lo, G.Y.-S. Vibrational Spectra of BrO<sup>-</sup>, BrO<sub>2</sub><sup>-</sup>, Br<sub>3</sub><sup>-</sup>, and Br<sub>5</sub><sup>-</sup>. *Inorg. Chem.* **1967**, *6*, 1483–1486. [[CrossRef](#)]
46. Devillanova, F.A.; Deplano, P.; Isaia, F.; Lippolis, V.; Mercuri, M.L.; Piludu, S.; Verani, G.; Demartin, F. Crystal structure and vibrational characterization of the reaction products of N-methylthiazolidine-2-(<sup>3</sup>H)-selone (1) and N-methylbenzothiazole-2-(<sup>3</sup>H)-selone (2) with Br( $\infty$ )<sub>2</sub>( $\infty$ ). *Polyhedron* **1998**, *17*, 305–312. [[CrossRef](#)]
47. Reich, O.; Hasche, S.; Büscher, K.; Beckmann, I.; Krebs, B. New oxonium bromochalcogenates(IV)—Synthesis, structure, and properties of [H<sub>3</sub>O][TeBr<sub>5</sub>] · 3C<sub>4</sub>H<sub>8</sub>O<sub>2</sub> and [H<sub>3</sub>O]<sub>2</sub>[SeBr<sub>6</sub>] | Neue oxonium-bromochalkogenate(IV)—Darstellung. *Z. Anorg. Allg. Chem.* **1996**, *622*, 1011–1018. [[CrossRef](#)]
48. Hendra, P.J.; Jović, Z. The Raman spectra of some complex anions of formula [MX( $\infty$ )<sub>6</sub>( $\infty$ )]<sup>2-</sup> in the solid phase and in solution, where M = Se and Te; X = Cl, Br, and I. *J. Chem. Soc. A Inorg. Phys. Theor.* **1968**, 600–602. [[CrossRef](#)]
49. Usoltsev, A.N.; Adonin, S.A.; Abramov, P.A.; Novikov, A.S.; Shayapov, V.R.; Plyusnin, P.E.; Korolkov, I.V.; Sokolov, M.N.; Fedin, V.P. 1D and 2D Polybromotellurates(IV): Structural Studies and Thermal Stability. *Eur. J. Inorg. Chem.* **2018**, *2018*, 3264–3269. [[CrossRef](#)]

50. Ivanov, D.M.; Baykov, S.V.; Novikov, A.S.; Romanenko, G.; Bokach, N.A.; Evarestov, R.A.; KuKushkin, V.Y. Noncovalent Sulfoxide-Nitrile Coupling Involving Four-Center Heteroleptic Dipole-Dipole Interactions between the Sulfinyl and Nitrile Groups. *Cryst. Growth Des.* **2020**, *20*, 3417–3428. [[CrossRef](#)]
51. Rozhkov, A.V.; Novikov, A.S.; Ivanov, D.M.; Bolotin, D.S.; Bokach, N.A.; Kukushkin, V.Y. Structure-Directing Weak Interactions with 1,4-Diodotetrafluorobenzene Convert One-Dimensional Arrays of  $[M^{II}(\text{acac})_2]$  Species into Three-Dimensional Networks. *Cryst. Growth Des.* **2018**, *18*, 3626–3636. [[CrossRef](#)]
52. Eliseeva, A.A.; Ivanov, D.M.; Novikov, A.S.; Rozhkov, A.V.; Korniyakov, I.V.; Dubovtsev, A.Y.; Kukushkin, V.Y. Hexaiododiplatinate(ii) as a useful supramolecular synthon for halogen bond involving crystal engineering. *Dalt. Trans.* **2020**, *49*, 356–367. [[CrossRef](#)]
53. Eliseeva, A.A.; Ivanov, D.M.; Novikov, A.S.; Kukushkin, V.Y. Recognition of the  $\pi$ -hole donor ability of iodopentafluorobenzene—a conventional  $\sigma$ -hole donor for crystal engineering involving halogen bonding. *CrystEngComm* **2019**, *21*, 616–628. [[CrossRef](#)]
54. Il'in, M.V.; Bolotin, D.S.; Novikov, A.S.; Kolesnikov, I.E.; Suslonov, V.V. Platinum(II)-mediated aminonitrone–isocyanide interplay: A new route to acyclic diaminocarbene complexes. *Inorg. Chim. Acta* **2019**, *490*, 267–271. [[CrossRef](#)]
55. Bader, R.F.W. A quantum theory of molecular structure and its applications. *Chem. Rev.* **1991**, *91*, 893–928. [[CrossRef](#)]
56. Espinosa, E.; Alkorta, I.; Elguero, J.; Molins, E. From weak to strong interactions: A comprehensive analysis of the topological and energetic properties of the electron density distribution involving X–H  $\cdots$  F–Y systems. *J. Chem. Phys.* **2002**, *117*, 5529–5542. [[CrossRef](#)]
57. Johnson, E.R.; Keinan, S.; Mori-Sánchez, P.; Contreras-García, J.; Cohen, A.J.; Yang, W. Revealing Noncovalent Interactions. *J. Am. Chem. Soc.* **2010**, *132*, 6498–6506. [[CrossRef](#)] [[PubMed](#)]
58. Contreras-García, J.; Johnson, E.R.; Keinan, S.; Chaudret, R.; Piquemal, J.P.; Beratan, D.N.; Yang, W. NCIPLOT: A program for plotting noncovalent interaction regions. *J. Chem. Theory Comput.* **2011**, *7*, 625–632. [[CrossRef](#)]
59. Bartashevich, E.V.; Tsirelson, V.G. Interplay between non-covalent interactions in complexes and crystals with halogen bonds. *Russ. Chem. Rev.* **2014**, *83*, 1181–1203. [[CrossRef](#)]